

VOLS. 65-66
Completing vols. 65-66

JUNE 2000

ISSN 0378-3820



Fuel Processing Technology

Special Issue

Air Quality:
Mercury, Trace Elements
and Particulate Matter



www.elsevier.com/locate/fuproc

UNIVERSITY OF PITTSBURGH

JUN 23 2000

BEVIER ENGINEERING LIBRARY

FUEL PROCESSING TECHNOLOGY

An international journal devoted to the processing and beneficiation of coal, petroleum, oil shale, tar sands and peat

FUEL PROCESSING TECHNOLOGY

Editor

Geoffrey P. Hoffman,
Lexington, KY, USA

Regional Editor for Europe

A.H. Memon
Zagreb, Czech

Regional Editor for The Far East

Peng Chen,
Beijing, P.R. China

Honorary Editor

Larry L. Anderson,
St. George, UT, USA

An international journal devoted to all aspects of processing and beneficiation of coal, petroleum, oil shale, tar sands and peat

Volumes 65-66 (2000)

Editorial Board

S.A. Beynon, Great Falls, NE, USA

J.C. Crilling, Cantonville, IL, USA

E. Ekin, Istanbul, Turkey

H.A. Gopal, New York, NY, USA

W.R. Jackson, Clayton, Vic., Australia

J. Ju, Beijing, P.R. China

L.A. Kuvshinov, Kemerovo, Russia

B. Li, Taiyuan, P.R. China

R. Markovskii, Des Plaines, IL, USA

A. Mavrou, Greece, Poland

T.C. Min, Ann Arbor, MI, USA

Y. Niirayama, Sendai, Japan

M. Nomura, Osaka, Japan

Y. Saito, Tsukuba, Japan

H.H. Schober, University Park, PA, USA

H. Schurr, Karlsruhe, Germany

A. Tanihara, Sendai, Japan

C. Wondol, Pittsburgh, PA, USA

W.H. Wiss, Salt Lake City, UT, USA

X. G. Yao, Taiyuan, P.R. China

Y. Yurum, Ankara, Turkey



ELSEVIER

Amsterdam - Lausanne - New York - Oxford - Shannon - Tokyo

Volumes 65-66 (2000)



Towards the development of a chemical kinetic model for the homogeneous oxidation of mercury by chlorine species

Rebecca N. Sliger^a, John C. Kramlich^{a,*}, Nick M. Marinov^b

^a Department of Mechanical Engineering, University of Washington, Box 352600, Seattle, WA 98195-2600, USA

^b Chemical Sciences Division, L-353, Lawrence Livermore National Laboratory, P.O. Box 808, Livermore, CA 94550, USA

Received 28 April 1999; accepted 20 August 1999

Abstract

The potential for regulation of mercury emissions from coal-fired boilers is a concern for the electric utility industry. Field data show a wide variation in the fraction of mercury that is emitted as a vapor vs. that retained in the solid products. The reason for this variation is not well-understood. Near the end of the flue gas path, mercury exists as a combination of elemental vapor and HgCl_2 vapor. The data show that HgCl_2 is more likely to be removed from the flue gas. Thus, the degree of oxidation is considered to be a critical factor that tends to reduce emission. Mercury is certain to exist as elemental vapor in the flame, with the oxidation occurring at some point in the post-flame environment. At present, the mechanism promoting this oxidation is not quantitatively known, particularly under the low chlorine concentrations afforded by many coals. In the present work, we measure mercury oxidation from a furnace operating between 860°C and 1171°C. These data are compared with similar results from the literature. The possible elementary reactions that may lead to oxidation are reviewed and a chemical kinetic model is proposed. This model yields good qualitative agreement with the data and indicates that mercury oxidation occurs during the thermal quench of the combustion gases. The model also suggests that atomic chlorine is the key oxidizing species. The oxidation is limited to a temperature window between 700°C and 400°C that is defined by the overlap of (1) a region of significant superequilibrium Cl concentration, and (2) a region where oxidized mercury is favored by equilibrium. Above 700°C, reverse reactions effectively limit oxidized mercury concentrations. Below 400°C, atomic chlorine concentrations are too low to support further oxidation. The implication of these results are that homogeneous

* Corresponding author. Tel.: +1-206-543-5538; fax: +1-206-685-8047; e-mail: kramlich@u.washington.edu

oxidation is governed primarily by (1) HCl concentration, (2) quench rate, and (3) background gas composition. © 2000 Elsevier Science B.V. All rights reserved.

Keywords: Chemical kinetic model; Oxidation; Mercury chloride; Emission

1. Introduction

The emission of mercury by coal-fired power plants has become a recent concern on the part of the electric utility industry. Title III of the 1990 Clean Air Act Amendments lists mercury as a hazardous air pollutant, and may subject industry to emission regulation, possibly leading to the need for emission controls. Field studies show that coal-fired plants emit anywhere from 5% to 95% of the mercury contained in their coal [1,2]. The reasons for this variability are poorly understood, but appear to involve the oxidation state of the mercury, the properties of the mineral matter associated with the coal, and the type of existing air pollution control equipment installed on the furnace. The heart of the problem is that the fundamental pathways governing the fate of mercury in the furnace environment are not known. These fundamental processes will, however, ultimately determine whether mercury is retained with the ash or emitted with the stack gas.

Oxidized mercury from coal combustion is generally thought to be HgCl_2 . Relative to elemental mercury, HgCl_2 is slightly less volatile at stack temperatures and below. A key difference is that HgCl_2 is water-soluble and that it tends to interact with mineral matter and char, and with cold-end air pollution control equipment. This is believed to be the source of the positive correlation between the fraction of mercury in the oxidized state and removal of mercury from the flue gas [3]. Thus, the factors that control the division of mercury between the elemental and oxidized states are thought to be of critical importance in understanding mercury emission behavior.

The literature clearly shows that homogeneous oxidation pathways exist [4–6]. In addition, heterogeneous processes are also considered to be important contributors in some regimes, either via promoting direct oxidation or by catalytically generating reactants for homogeneous oxidation [7]. In any case, an accurate homogeneous oxidation mechanism is needed as a component in any overall model of the fate of mercury in coal combustion furnaces. The present work focuses on this goal.

2. Overview of mercury oxidation behavior

Mercury is of sufficiently high volatility that it is presumed to completely vaporize in the flame irrespective of its original form [8]. At flame temperatures, equilibrium indicates mercury will exist in the elemental state. As temperatures fall, the favored equilibrium product shifts to HgCl_2 . Fig. 1 shows equilibrium partitioning between Hg and HgCl_2 for three HCl concentrations (50, 500, and 3000 ppm, the latter being representative of waste incineration). (These calculations make use of the thermochemical database used for the kinetic calculations, described below. They are based on the

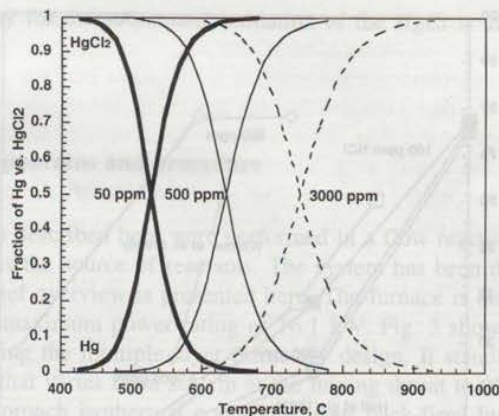
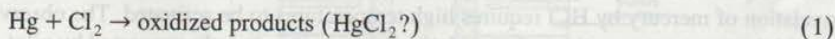


Fig. 1. Equilibrium distribution of elemental and oxidized mercury for various HCl concentrations.

nominal reactor gas composition, also listed below.) The crossover temperature between the elemental and oxidized forms increases from 530° to 740°C as the background HCl concentration goes from 50 to 3000 ppm. This crossover point is not influenced by mercury concentration as long as hydrochloric acid is present in excess, which is the usual case. At low temperatures, approximately 10% of the mercury is predicted to be present as HgO. These trends are consistent with reports in the literature [8,9].

Kinetic data for the oxidation of elemental mercury under appropriate conditions are sparse. Results have been obtained for the direct reaction of $\text{Hg} + \text{Cl}_2$ in a flow reactor experiment in the absence of any other species [5]. The results were obtained by varying the Cl_2 concentration and observing the extent of oxidation at the exit. The conversion was independent of temperature between 20°C and 700°C, and was essentially complete when the Cl_2 concentration reached 10 ppm. These data can be reduced to yield a second order rate constant:



with $k_1 = 3.4 \times 10^9 \text{ cm}^3/\text{mol s}$. A similar experiment was performed at 500°C using flue gas as the background for the reaction. In this case, the extent of oxidation was substantially reduced (e.g., to only 25% at 10 ppm Cl_2). This suggests the presence of the flue gas constituents (e.g., CO_2 , H_2O , O_2) interfere in the mercury oxidation process.

The elementary reaction $\text{Hg} + \text{HCl}$ is hindered by a very high energy barrier and cannot be considered as an important path under practical conditions [10]. A limited number of studies have, however, examined the global reaction. Fig. 2 shows flow reactor results from Hall et al. [5] and Widmer et al. [6]. The Hall results are under 10% O_2 and an initial Hg concentration of 100 $\mu\text{g}/\text{m}^3$, while the Widmer results are under a simulated flue gas and 3000 $\mu\text{g}/\text{m}^3$ initial Hg. The Hall results show mercury oxidation increasing with temperature, at least to 900°C. This is in apparent contradiction to the equilibrium results of Fig. 1, which shows that at these temperatures elemental mercury

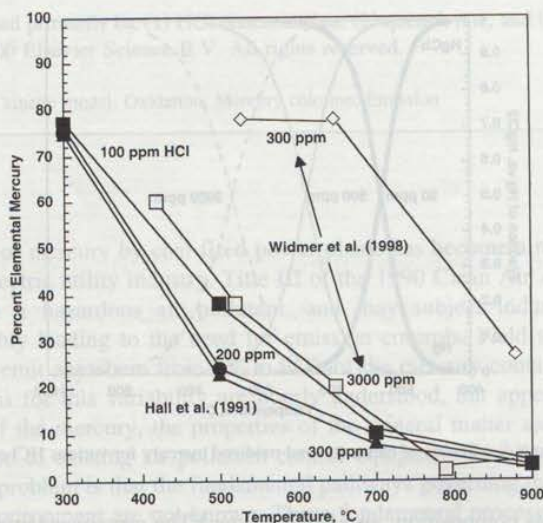


Fig. 2. Comparison of literature data on oxidation from flow reactors: Hall et al. [5] and Widmer et al. [6].

is the exclusive form. The influence of chlorine concentration is weak. The Widmer experiments show a similar superequilibrium yield of oxidized mercury at high temperatures, although the yields are lower than those for the corresponding Hall conditions. At least two possible reasons attach themselves to the lower reactivity of the Widmer experiments: (1) as with the Cl_2 results, the inclusion of H_2O or CO_2 in the reactants appears to reduce the extent of oxidation, or (2) the higher Hg concentration of the Widmer experiments results in less mercury oxidation.

This figure shows that (1) oxidation apparently occurs well above the temperatures at which equilibrium would predict only elemental mercury should exist, and (2) the global oxidation of mercury by HCl requires high temperatures to be activated. The observation that high temperatures activate the oxidation reaction is indirectly supported by pilot-scale data [11]. In two sets of tests, chlorine was added to improve HgCl_2 production and spray dryer performance. The chlorine was first added as NaCl with the coal, which resulted in a substantial improvement in performance. In another series, the chlorine was added as HCl at 540°C in the flue gas, which showed a severe reduction in conversion and capture. These results support the idea that moderately high temperatures are needed to affect reaction.

One such pathway involves chlorine atom. As will be discussed presently, the rate of the reaction:



has been measured [12]. This low energy barrier reaction proceeds at room temperature near the collision limit, and its rate constant shows little apparent temperature depen-

dence. The pathway for the subsequent oxidation of the HgCl is uncertain and will be addressed later.

3. Experimental apparatus and procedure

The experiments described here were performed in a flow reactor system that uses a natural gas flame as the source of reactants. The system has been described previously [13], and only a brief overview is presented here. The furnace is down-fired on natural gas and air with a maximum power rating of 16.1 kW. Fig. 3 shows a cross-section of the furnace, including the multiple layer refractory design. It stands 2.4 m tall, with a flowpath diameter that varies from 2.5 cm at the mixing throat to 20 cm in the body of the furnace. To approach isothermal conditions, four back-fired burners, forming two pairs of heating channels, are used along the middle section of the furnace. Sample

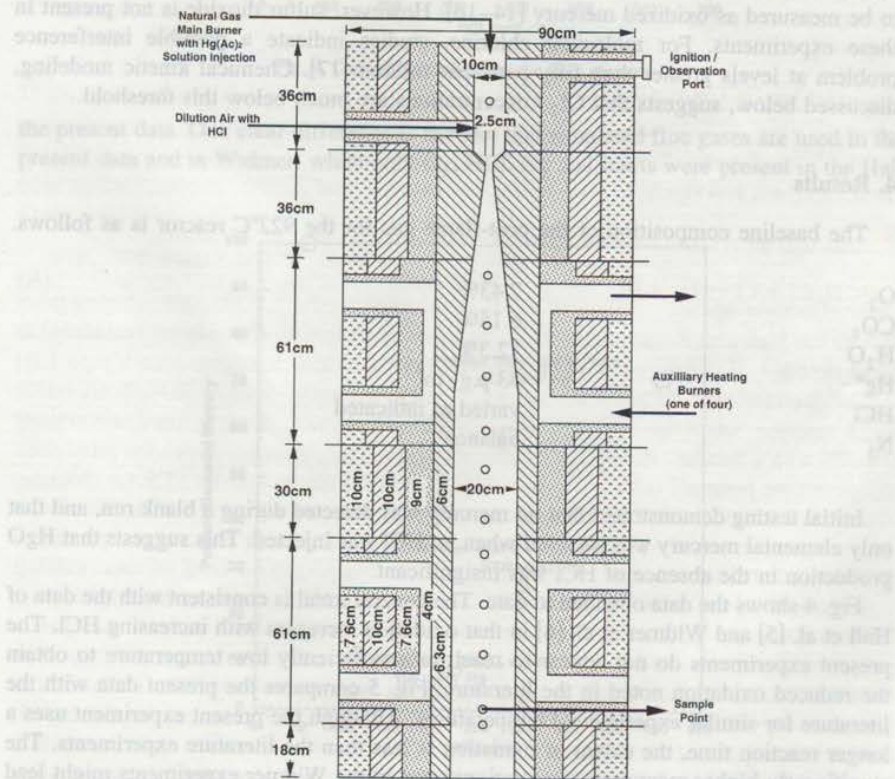


Fig. 3. Experimental system schematic.

ports, shown along the center of the furnace, allow for gas extraction; the second-to-lowest sampling port is used in the present study.

During testing, a mercuric acetate solution is atomized into the primary flame. The high temperature of the flame ensures that the acetate is decomposed and the mercury is reduced to its elemental form. The latter point has been verified by injecting mercury in the absence of hydrochloric acid; measurements show the entire recovery to be elemental rather than oxidized mercury. The injection solution should be acidified with nitric acid to prevent mercury precipitation, which can lead to reproducibility problems with injection rate.

A lance is used to inject the gaseous HCl as shown on the figure. Variations in the stoichiometry of the main burner bring the gases to the desired temperature in the test section. The region between the HCl injection point and the sample probe inlet corresponds to the test section. For all cases, the residence time is approximately 1.4 s.

A simplification of EPA Method 29 is used to measure and speciate mercury (EPA, 1994). In the present experiments, a quartz probe is used without a filter since no particulate matter is present in the experiment. With this method the interferences are sulfur dioxide (SO₂) and molecular chlorine (Cl₂), which can cause elemental mercury to be measured as oxidized mercury [14–16]. However, sulfur dioxide is not present in these experiments. For molecular chlorine, studies indicate a possible interference problem at levels greater than fifty parts per million [17]. Chemical kinetic modeling, discussed below, suggests that Cl₂ concentrations are much below this threshold.

4. Results

The baseline composition of the post-flame gas for the 922°C reactor is as follows.

O ₂	7.43%
CO ₂	6.15%
H ₂ O	12.3%
Hg ^o	53 μg/m ³
HCl	varied as indicated
N ₂	balance

Initial testing demonstrated that no mercury was detected during a blank run, and that only elemental mercury was detected when no HCl was injected. This suggests that HgO production in the absence of HCl was insignificant.

Fig. 4 shows the data obtained to date. The general trend is consistent with the data of Hall et al. [5] and Widmer et al. [6] in that oxidation increases with increasing HCl. The present experiments do not appear to reach to a sufficiently low temperature to obtain the reduced oxidation noted in the literature. Fig. 5 compares the present data with the literature for similar experimental temperatures. Although the present experiment uses a longer reaction time, the extent of oxidation is less than the literature experiments. The significantly higher mercury concentrations used in the Widmer experiments might lead to less oxidation, if any change were to occur. The Widmer oxidation, however, exceeds

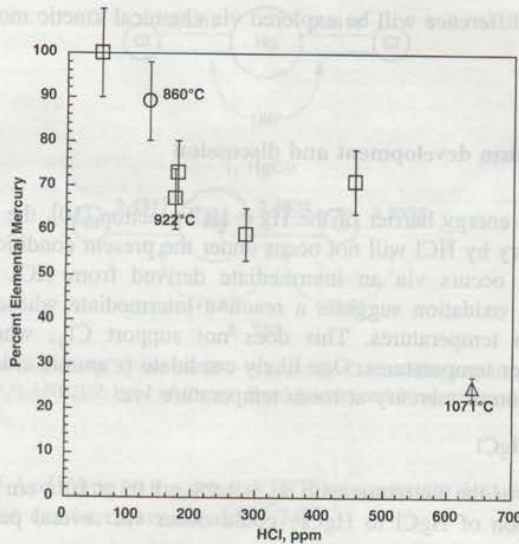


Fig. 4. Oxidation results from the flow reactor.

the present data. One clear difference is the fact that simulated flue gases are used in the present data and in Widmer, while only O₂, HCl, Hg and inerts were present in the Hall

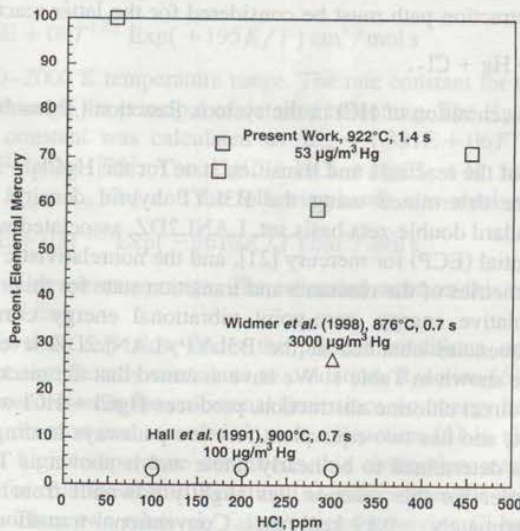


Fig. 5. Comparison of the present data with literature results (Hall et al. [5] and Widmer et al. [6]) in the neighborhood of 900°C.

experiments. This difference will be explored via chemical kinetic modeling in Section 5.

5. Kinetic mechanism development and discussion

Due to the high energy barrier of the $\text{Hg} + \text{HCl}$ reaction [10], the direct elementary oxidation of mercury by HCl will not occur under the present conditions. This suggests that the oxidation occurs via an intermediate derived from HCl. The temperature dependence of the oxidation suggests a reactive intermediate whose concentration is promoted by high temperatures. This does not support Cl_2 , whose concentration increases with lower temperatures. One likely candidate is atomic chlorine.

The fast oxidation of mercury at room temperature via:



has been reported in the literature with $k_2 = 1.95 \pm 1.05 \times 10^{13} \text{ cm}^3/\text{mol s}$ [12]. The subsequent oxidation of HgCl to HgCl_2 could occur via several paths, including the following.



Although an abstraction path must be considered for the latter reaction:



Due to the high concentration of HCl in the system, Reaction (3) has been considered in some detail.

The geometries of the reactants and transition state for the $\text{HgCl}_2 + \text{H} \rightarrow \text{HgCl} + \text{HCl}$ (k_{3b}) reaction were determined using the B3LYP hybrid density functional theory [18–20] with a standard double-zeta basis set, LANL2DZ, associated with the relativistic effective core potential (ECP) for mercury [21], and the nonrelativistic ECP for chlorine. The optimized geometries of the reactants and transition state for this reaction are shown in Fig. 6. The relative energy, zero-point vibrational energy correction, rotational constants, and frequencies obtained at the B3LYP/LANL2DZ level of theory using Gaussian98 [22] are shown in Table 1. We have assumed that the reaction of HgCl_2 with H-atom occurs by direct chlorine abstraction, produces $\text{HgCl} + \text{HCl}$ without involving a long-lived complex, and has two equivalent reaction pathways leading to products. The transition state was determined to be nearly linear and is shown as TS1 in Fig. 6. The critical energy barrier for this reaction lies slightly downhill from the HgCl_2 and H reactants by approximately -0.19 kcal/mol . Conventional transition state theory was employed to calculate the rate constant for the $\text{HgCl}_2 + \text{H} \rightarrow \text{HgCl} + \text{HCl}$ reaction. The calculation was based on the critical energy computed using the B3LYP hybrid density

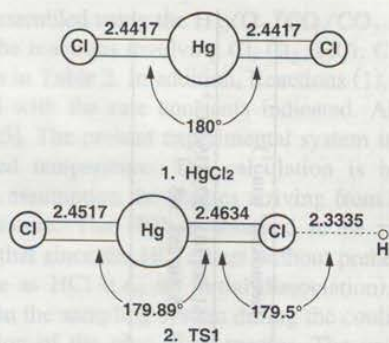


Fig. 6. Optimized geometries of HgCl₂ and the H···Cl···Hg-Cl transition state involved in the HgCl₂ + H reaction at the B3LYP/LANL2DZ level of theory. Bond lengths and bond angles are in ångström (Å) and degree (°), respectively.

functional method. According to the general TST, rate constant k at temperature T for a bimolecular reaction can be expressed as [23,24]

$$k(T) = L^\ddagger k_B T / h \exp(-\Delta G^\ddagger(T) / k_B T).$$

The L^\ddagger is the statistical factor which accounts for the number of equivalent reaction pathways; h is the Planck's constant; k_B is Boltzmann constant; and $\Delta G^\ddagger(T)$ is the standard-state free energy of activation change at temperature, T , going from the initial state to the transition state. A least squares analysis of the calculated rate constants leads to the following rate expression

$$k_{3b} = 6.406E + 09T^{1.02} \text{Exp}(+195K/T) \text{ cm}^3/\text{mol s}$$

valid over the 900–2000 K temperature range. The rate constant for the reverse reaction may be obtained through the principal of detailed balancing. The HgCl₂ + H ↔ HgCl + HCl equilibrium constant was calculated as $K_{\text{eq}} = 1.381E + 06T^{-1.48} \text{Exp}(9811/T)$ from the JANAF tables [25]. The HgCl + HCl → HgCl₂ + H rate expression was determined from $K_{\text{eq}} = k_{3b}/k_{3f}$ and the following result was obtained

$$k_{3f} = 4.638E + 03T^{2.5} \text{Exp}(-9616K/T) \text{ cm}^3/\text{mol s}$$

for the 900–2000 K temperature range. The estimated error on this rate constant is plus or minus a factor of four.

This reaction is thus very slow under the present conditions, and as will be seen presently, does not significantly contribute to oxidation. Reaction (5) is exothermic and is expected to proceed at near the collisional limit since no energy barrier is present for addition. For this reaction we assumed $k_5 = k_2$. Reaction (6) is also exothermic (33 kcal/mol), and at high temperature conditions this abstraction reaction may compete with Reaction (5) for chlorine atoms. Reaction (4) suffers from the absence of Cl₂ under high temperatures. Thus, two relatively fast reactions involving Cl have the potential to oxidize mercury at any temperature. If so, the key to predicting homogeneous mercury oxidation is to predict chlorine atom behavior.

Table 1
Relative energies, zero-point energy correction, rotational constants, and frequencies of reactants and transition state

Species	Relative energy (in hartree)	Zero-point energy correction (in hartree)	Rotational constants (cm ⁻¹)	Frequencies ^a (cm ⁻¹)
H...Cl...Hg-Cl	-73.2150355	0.001986	22,200.26; 0.03782; 0.03782	61, 90, 103, 283, 335, 2471 ^b
Cl-Hg-Cl	-72.7158256	0.000521	0.0; 0.03782; 0.03782	66, 66, 288, 345
H	-0.4989111	-	-	-

^aFrequencies are not scaled.

^bDenotes the imaginary frequency.

A mechanism was assembled using the $H_2/O_2/CO/CO_2$ reaction set from Warnatz et al. [26], along with the reactions involving Cl, Cl_2 , HCl, ClO, HOCl, from the NIST data base [27], as shown in Table 2. In addition, Reactions (1), (2), (3), and (5) involving mercury were included with the rate constants indicated. All cases used the JANAF thermochemical data [25]. The present experimental system is modeled as a plug-flow reactor at the measured temperature. The calculation is initialized at the chlorine injection point with the assumption the species arriving from the flame are equilibrated at the injection temperature. The HCl is assumed to be rapidly dispersed into the post-flame gases. Note that since the HCl enters without preheating, the calculations are started with all chlorine as HCl (i.e., no initial dissociation). Due to the potential for continued reaction within the sampling system during the cooling of the gases, the probe is treated as an extension of the plug-flow reactor. The probe temperature profile is calculated from heat transfer based on a constant wall temperature equal to that of the cooling medium. This results in a temperature profile that varies linearly from 922°C to 868°C over 1.4 s in the furnace, followed by a quench to room temperature at ~ 5400 K/s in the probe.

The results of the calculation are shown in Fig. 7. Analysis of the results indicates that the entire oxidation is due to $Hg + Cl \rightarrow HgCl$ and $HgCl + Cl \rightarrow HgCl_2$. Furthermore, the entire oxidation is taking place within the temperature quench environment provided by the sample probe. Fig. 8 shows time resolved behavior of both mercury and Cl within the quench. At the inlet to the quench region, mercury is in its elemental equilibrium state. The shallow temperature decline in the furnace causes a decrease in equilibrium Cl, while kinetic constraints on recombination maintain the calculated Cl somewhat above the equilibrium value at the probe inlet. The rapid quench coupled with

Table 2
Kinetic data from NIST database (units: cm, mol, s; for E, kcal/mol)

				A	n	E	
Cl	Cl	M \rightarrow Cl ₂	M	14.400	0.0	-1.8	
H	Cl	M \rightarrow HCl	M	17.000	0.0	0.0	
HCl	H	\rightarrow H ₂	Cl	13.360	0.0	3.5	
H	Cl ₂	\rightarrow HCl	Cl	13.930	0.0	1.2	
O	HCl	\rightarrow OH	Cl	3.53	2.87	3.51	
OH	HCl	\rightarrow Cl	H ₂ O	7.43	1.65	-0.223	
O	Cl ₂	\rightarrow ClO	Cl	12.790	0.0	3.585	
O	ClO	\rightarrow Cl	O ₂	13.2	0.0	-0.193	
Cl	HO ₂	\rightarrow HCl	O ₂	13.030	0.0	0.894	
Cl	HO ₂	\rightarrow OH	ClO	13.39	0.0	-0.338	
Cl	H ₂ O ₂	\rightarrow HCl	HO ₂	12.800	0.0	1.951	
ClO	H ₂	\rightarrow HOCl	H	11.78	0.0	14.1	
H	HOCl	\rightarrow HCl	OH	13.980	0.0	7.62	
Cl	HOCl	\rightarrow HCl	ClO	12.260	0.0	0.258	
Cl ₂	OH	\rightarrow Cl	HOCl	12.100	0.0	1.81	
O	HOCl	\rightarrow OH	ClO	12.780	0.0	4.372	
OH	HOCl	\rightarrow H ₂ O	ClO	12.255	0.0	0.994	
HOCl		M \rightarrow OH	Cl	M	10.250	-3.0	56.72

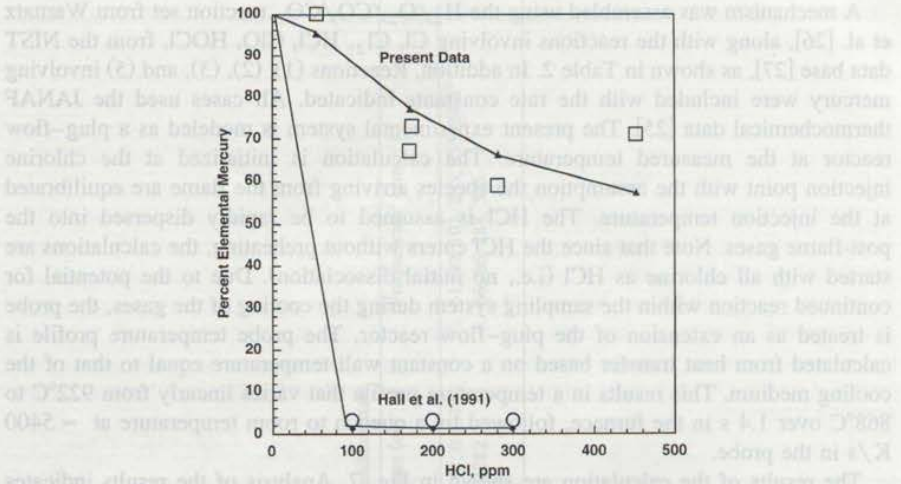


Fig. 7. Comparison of data with predictions from the kinetic model (literature: Hall et al. [5]).

kinetic constraints on recombination cause the chlorine atom to hold a significant superequilibrium concentration. This, coupled with the slowing of the reverse of equilibrium state. The shallow temperature decline in the furnace causes a decrease in equilibrium Cl while some recombination remains the calculated Cl somewhat above the equilibrium level.

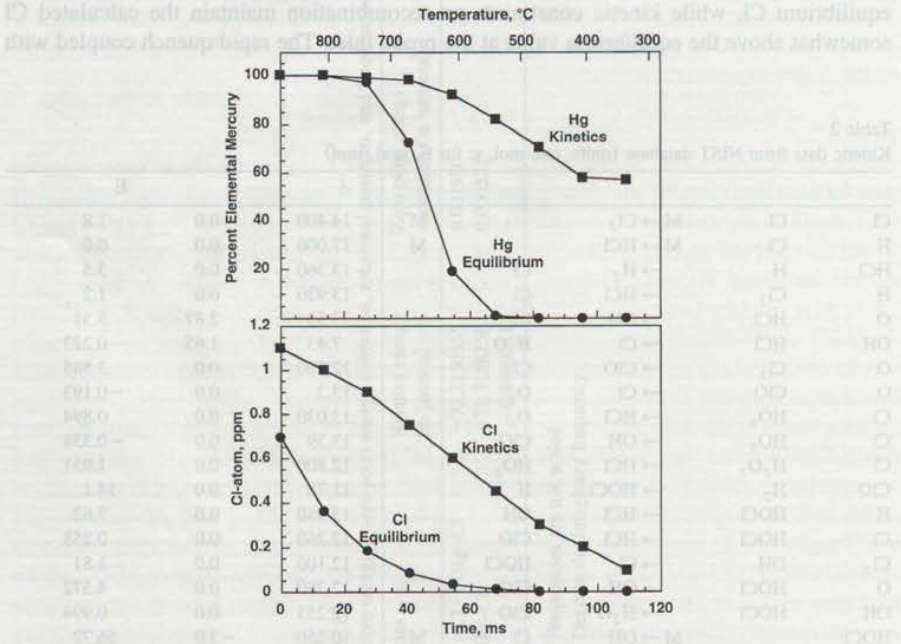


Fig. 8. Time resolved predictions within the quench zone for the 922°C, 453 ppm initial HCl case.

Reactions (2) and (5), leads to oxidation. Note from the figure that the oxidation proceeds within a window associated with the overlap of (1) significant superequilibrium Cl (for $T > 400^\circ\text{C}$), and (2) HgCl_2 as a favored equilibrium product (for $T < 700^\circ\text{C}$). This scenario suggests that identical oxidation extents would be observed independently of furnace temperature as long as the furnace was above $\sim 850^\circ\text{C}$ and the initial gas composition was fixed.

The influence of quench rate was investigated by repeating the calculation while adjusting the quench rate downward from the 5400 K/s that is characteristic of the probe. (Note that the lower quench rates shown on the figure encompass rates found in practical furnaces.) The results, shown in Fig. 9, indicate that slower quench initially leads to increased oxidation, followed by reduced oxidation. Analysis of the kinetics shows that very short quench times limit the oxidation via reduced time available for reaction. Very long times allow the Cl to more closely follow equilibrium, effectively reducing the imbalance between oxidation and reduction directions of Reactions (2) and (5).

The principal reaction removing Cl is the recombination $\text{Cl} + \text{Cl} + \text{M} \rightarrow \text{Cl}_2 + \text{M}$, and the results are most dependent on the rate constant of this reaction. The recombination yields Cl_2 , which can react with mercury according to Reaction (1). There is, however, insufficient time for Reaction (1) to make use of this Cl_2 for oxidation under the current configuration. A long residence time at 300 K following the quench could, however, lead to more oxidation.

Analysis of the kinetics indicates that the injected HCl becomes rapidly equilibrated with Cl, suggesting that there is no difference between the present experiment and (1) experiments such as Hall et al. [5], and Widmer et al. [6] where the HCl is preheated, and (2) practical furnaces where both mercury and chlorine are exposed to flame temperatures. Instead, the downstream environment, specifically quench and composition, appear to be the critical characteristics.

Fig. 7 also shows model results for the Hall et al. [5] experiment. The calculations were obtained with the assumptions (1) that the product gases from the isothermal zone were cooled before the analyzer at the same rate as in the present experiment (5400

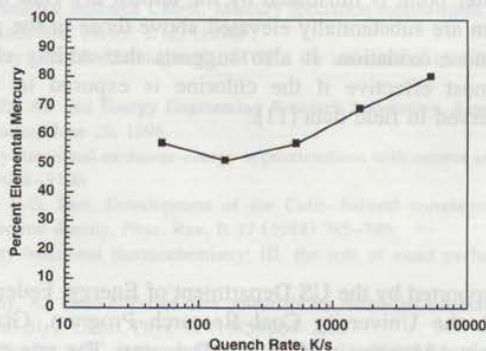


Fig. 9. Chemical kinetic model results on the influence of quench rate on mercury oxidation.

K/s), and (2) that the reacting gases were equilibrated in the high-temperature furnace. Since the reactants contain just Hg, O₂, N₂ and HCl, the only water present was the result of HCl decomposition. In this environment, the equilibrium Cl concentration is substantially higher than in the present experiment. For example, at 900°C and 300 ppm HCl, equilibrium under the present experimental composition yields 0.54 ppm Cl, while under the Hall experiment the yield is 21 ppm. This is the cause of much higher oxidation noted in the model runs. As with the model of our experiment, all the oxidation is occurring during sample quench.

Finally, it should be noted that the mechanism proposed here is likely not to be the only means of oxidizing mercury in practical systems. An alternate (and possibly concurrent) oxidation mechanism has been proposed for much lower temperatures [7]. This is based on the Cl₂ reaction (Reaction (1)). Here, Cl₂ is catalytically generated by the interaction of HCl with fly ash and char. Once formed, the Cl₂ rapidly reacts with the Hg, and the oxidized mercury is partially captured by the char. This idea originates from mechanisms developed to explain the formation of chlorinated dibenzo-*p*-dioxins in downstream incineration equipment.

6. Conclusions

A number of experiments, including the present data, suggest that mercury oxidation occurs at temperatures above the point where equilibrium predicts only elemental mercury will exist. Examination of possible elementary reactions indicates that only reactions with Cl are fast enough to account for the oxidation. Chemical kinetic modeling of the reaction environment, including the inevitable quench that must precede analysis (which occurs either in a probe or in the furnace), suggests that the oxidation occurs within a window between 700° and 400°C that is the result of the overlap of (1) a region of superequilibrium Cl concentration, and (2) a region where oxidized mercury is favored by equilibrium. The implication of these results are that homogeneous oxidation is governed primarily by (1) HCl concentration, (2) quench rate, and (3) background gas composition. The latter point is illustrated by the almost dry Hall data, where equilibrium Cl concentration are substantially elevated above those in the present experiment, resulting in much more oxidation. It also suggests that adding chlorine to improve oxidation will be most effective if the chlorine is exposed to a high-temperature environment, as observed in field data [11].

Acknowledgements

This work was supported by the US Department of Energy, Federal Energy Technology Center, through the University Coal Research Program, Grant No. DE-FG22-95PC95216. The Project Monitor is Mr. Louis Dalverny. The rate constant calculations were performed under the auspices of the US Department of Energy by the Lawrence

Livermore National Laboratory under contract No. W-7405-ENG-48. Mr. David Going performed several preliminary kinetic calculations in support of this work.

References

- [1] C. Jones, Consensus on air toxics eludes industry to date, *Power* 138 (1994) 51–59, October.
- [2] W. Chow, M.J. Mill, I.M. Torrens, Pathways of trace elements in power plants: interim research results and implications, *Fuel Process. Technol.* 39 (1994) 5–20.
- [3] R. Meij, The fate of mercury in coal-fired power plants and the influence of wet flue-gas desulphurization, *Water, Air, Soil Pollut.* 56 (1991) 21–33.
- [4] B. Hall, O. Lindqvist, E. Ljungström, Mercury chemistry in simulated flue gases related to waste incineration conditions, *Environ. Sci. Technol.* 24 (1990) 108–111.
- [5] B. Hall, P. Schager, O. Lindqvist, Chemical reactions of mercury in combustion flue gases, *Water, Air, Soil Pollut.* 56 (1991) 3–14.
- [6] N.C. Widmer, J.A. Cole, W.R. Seeker, J.A. Gaspar, Practical limitation of mercury speciation in simulated municipal waste incinerator flue gas, *Combust. Sci. Technol.* 134 (1998) 315–326.
- [7] C.L. Senior, L.E. Bool, G.P. Huffman, F.E. Huggins, N. Shaw, A. Sarofim, I. Olmez, T. Zeng, A fundamental study of mercury partitioning in coal fired power plant flue gas, Air and Waste Management Association's 90th Annual Meeting and Exhibition, 97-WP72B.08, June 1997.
- [8] R. Rizeq, D. Hansell, W. Seeker, Predictions of metals emissions and partitioning in coal-fired combustion systems, *Fuel Process. Technol.* 39 (1994) 219–236.
- [9] B.K. Gullett, Sorbent injection for dioxin/furan prevention and mercury control, Multipollutant Sorbent Reactivity Workshop, Research Triangle Park, NC, July 1994.
- [10] J. Hranisavljevic, A. Fontijn, Kinetics of ground-state Cd reactions with Cl_2 , O_2 , and HCl over wide temperature ranges, *J. Phys. Chem.* 101 (1997) 2323–2326.
- [11] R. Gleiser, K. Felsvang, Mercury emission reduction using activated carbon with spray dryer flue gas desulfurization, *Proc. Am. Power Conf.* 56 (1994) 452–457.
- [12] D.G. Horne, R. Gosavi, O.P. Strausz, Reactions of metal atoms: I. The combination of mercury and chlorine atoms and the dimerization of HgCl , *J. Chem. Phys.* 48 (1968) 4758–4764.
- [13] B.C. Chenevert, J.C. Kramlich, K.M. Nichols, Ash characteristics of high alkali sawdust and sanderdust biomass fuels, 27th Symposium (International) on Combustion, The Combustion Institute, Pittsburgh, 1998, pp. 1719–1725.
- [14] P. Chu, D.B. Porcella, Mercury stack emissions from US electric utility power plants, *Water, Air, Soil Pollut.* 80 (1995) 135–144.
- [15] Energy and Environmental Research Center, Mercury speciation measurement project continuing at the EERC, *Cent. Air Toxic Met. Newsl.* 2 (2) (1996).
- [16] C. Krivanek, Mercury control technologies for MWCs: the unanswered questions, *J. Hazard. Mater.* 47 (1996) 119–136.
- [17] W.P. Linak, US EPA Air and Energy Engineering Research Laboratory, Research Triangle Park, NC, personal communication, June 29, 1998.
- [18] A.D. Becke, Density-functional exchange-energy approximations with correct asymptotic behavior, *Phys. Rev. A* 38 (1988) 3098–3100.
- [19] C. Lee, W. Yang, R.G. Parr, Development of the Colle–Salvetti correlation-energy formula into a functional of the electron density, *Phys. Rev. B* 37 (1988) 785–789.
- [20] A.D. Becke, Density-functional thermochemistry: III. the role of exact exchange, *J. Chem. Phys.* 98 (1993) 5648–5652.
- [21] W.R. Wadt, P.J. Hay, Ab initio effective core potentials for molecular calculations. Potentials for main group elements Na to Bi, *J. Chem. Phys.* 82 (1985) 284–296.
- [22] M.J. Frisch, G.W. Trucks, H.B. Schlegel, G.E. Scuseria, M.A. Robb, M. Head-Gordon, P.M.W. Gill, M.W. Wong, J.B. Foresman, B.G. Johnson, R. Gomperts, J.L. Andres, K. Raghavachari, J.S. Binkley, C.

- Gonzales, R.L. Martin, D.J. Fox, D.J. DeFrees, J. Baker, E.S. Repogle, J.A. Pople, Gaussian98 Rev. A.4, Gaussian, Pittsburgh, PA, 1998.
- [23] K.A. Connors, Chemical Kinetics, VCH Publishers, New York, 1990, p. 200.
- [24] J.I. Steinfeld, J.S. Francisco, W.L. Hase, Chemical Kinetics and Dynamics, 2nd edn., Prentice-Hall, New York, 1999, p. 300.
- [25] M.W. Chase Jr., C.A. Davies, J.R. Downey Jr., D.J. Frurip, R.A. McDonald, A.N. Syverud, JANAF thermochemical tables, J. Phys. Chem. Ref. Data 14 (1985) 1–1856, Suppl. 1.
- [26] J. Warnatz, U. Maas, R.W. Dibble, Combustion, Springer, 1996, pp. 67–71.
- [27] NIST Chemical Kinetic Database: <http://www.csl.nist.gov/div836/ckmech.html/1999>.